Assembly of Carbon Dots Into Frameworks With Enhanced Stability and Antibacterial Activity

Pengfei Zhuang
Jinzhou Medical University
Kuo Li
The First Affiliated Hospital of Jinzhou Medical University
Daoyong Li
The first affiliated hospital of Jinzhou Medical University
Haixia Qiao
Jinzhou Medical University
Yifeng E
Jinzhou Medical University
Mingqun Wang
Jinzhou Medical University
Jiachen Sun
The First Affiliated Hospital of Jinzhou Medical University
Xifan Mei
The First Affiliated Hospital of Jinzhou Medical University
DAN LI (danli@jzmu.edu.cn)
Jinzhou Medical University

Nano Express

Keywords: Carbon dots1, Carbon Framworks2, Bacteria3, E. coli4, S. aureus5

Posted Date: May 6th, 2021

DOI: https://doi.org/10.21203/rs.3.rs-466450/v1

Version of Record: A version of this preprint was published at Nanoscale Research Letters on July 29th, 2021. See the published version at https://doi.org/10.1186/s11671-021-03582-3.

Abstract

Carbon dots (CDs) have widely been used as antimicrobials due to their active surface, but they also suffer instability. Therefore the relative applications such as the antibacterial activity may not be reliable for long-term use. Herein, we synthesize CDs with blue fluorescence by a hydrothermal process. Thereafter, polyethylenimine (PEI) was applied for the assembly of CDs into CDs-based frameworks (CDFs). The CDFs exhibited quenched fluorescence but showed more stable properties based on the scanning electron microscope (SEM) and zeta potential investigations. Both CDs and CDFs show antibacterial activity toward Gram-negative Escherichia coli (*E. coli*) and Gram-positive Staphylococcus aureus (*S. aureus*), but CDFs exhibited better antibacterial performance. This reveals CDFs magnify both the stability and antibacterial activity, which would be more promising for practical applications.

2. Materials And Methods

2.1 Materials and instrument

X-ray surface photoelectron spectra (XPS) were recorded on an ESCALAB250Xi X-ray surface photoelectron spectroscopy (XPS) instrument. The transmission electron microscope (TEM) was performed by a JEM-2100 microscope operating at 200 kV. The fluorescence of the materials was obtained using the F97 fluorescence spectrometer. The FDA/PI staining of the bacterial cells was recorded in tapping mode with a Leica DFC450C microscope. Fluorescence lifetime was measured on a time-correlated single-photon counting (TCSPC) system using a Nanolog spectrofluorometer (Horbia JY, Japan). Ultraviolet-visible spectroscopy (UV-vis) spectra are obtained from the UV-1600 instrument. All the reagents were of analytical grades. The deionized water was used through the experiments. Cell counting kit-8 was obtained from Beyotime Biotechnology.

2.2 Preparation of CDs and CDFs

L- cysteine (1.0 g) was dissolved in 10.0 mL of deionized water and mixed well. Then, the pH of the solution was adjusted to 9.0 with 1.0 M NaOH. The solution was transferred to a hydrothermal reactor and heated at 160°C for 24 hours. After the solution was cooled to room temperature, the resulting solution was subjected to dialysis using a dialysis bag (MW 7000 cut off) for one day. The as-obtained CDs were used for the following characterizations and experiments. For the preparation of CDFs, 40 μL of 1% PEI was added to 1 mL of the CDs. The mixture was allowed to stay for 1 hour. The product was purified by dialysis using the same method as the purification of CDs.

2.3 Toxicity evaluation

PC12 (a cell line obtained from a pheochromocytoma of the rat adrenal medulla) cells were seeded in 96-well plates for 12 hours and then were incubated with CDs and CDFs with different concentrations. The number of viable cells was investigated using a Cell Counting Kit-8 assay (CCK-8). MTT (5 mg/mL in PBS) was added at 1/10 culture volume, and the cells were returned to the incubator. After that, the supernatants were discarded and 200 μL of dimethyl sulfoxide (DMSO) was added to each well. The

crystals were dissolved by shaking the plates for 10 minutes. The absorbance at 490 nm was measured using the Microreader (Varioskan LUX Multimode Reader). Blank control wells were included for all the absorbance measurements.

2.4 Antibacterial Experiment

E. coli and *S. aureus* was incubated in the absence and presence of CDs and CDFs at 37°C with 250 rpm shake. Growth of the bacterial cells in Lysogeny broth (LB) culture was measured by the Microreader at 600 nm wavelength (OD600). LB medium was used as the blank control. The OD600 stands for the cell density and the relative cell viability was calculated based on the comparison between the cultured bacterial cells in the presence of the materials to the control group (OD600 of the bacterial cells in the absence of the CDs or CDFs). The live/dead bacteria are evaluated by the FDA/PI staining protocol. [17]

3. Results And Discussions

3.1. Characterization of the materials

3.1.1. SEM investigations

Figure 1 shows the SEM of the powder for CDs (Fig. 1a0) and CDFs (Fig. 1b0) after exposure to the air for several hours. It can be seen that the powders of CDs were irregular. On the other hand, the CDFs were well distributed and showed an average size of ca. 25 nm. CDs were supposed to show mono-dispersed small sizes based on the TEM study (Figure S1), but these small particles exhibited aggregation after exposing to air for a certain time. On the other hand, CDFs kept their morphology though they were exposed to the ambient environment. This indicated the as-obtained CDFs are more promising for practical applications. Because SEM could not show the high-resolution morphology of the materials, CDFs were further characterized by TEM (Fig. 1b1). It can be seen that CDFs exhibited assembly structure with small CDs as the building blocks. The assembly CDFs may combine the advantages of both the entire large frameworks and the interior small building blocks.

3.1.2. Zeta Potential

Zeta-potential investigations were used to measure the degree of electrostatic repulsion of CDs and CDFs between adjacent charged particles in the dispersed system (Fig. 3). It can be seen that the zeta-potential peak of CDs was not well featured, which were exposed to the ambient environment. Besides, unrepeatable zeta potential values were obtained when the same measurement was investigated another time, indicating the CDs were quite unstable. On the other hand, the zeta potential peak for CDFs was sharp and we had more repeatable data based on three times measurements, revealing CDFs were more stable and the dispersed systems had samples with higher purity.

3.1.3. Fluorescence properties

The fluorescence emission spectra were used to monitor the assembly process of CDs to CDFs. As the titration of PEI, the fluorescence emission at 350 nm gradually quenched. But no significant fluorescence spectra shift was observed, revealing no aggregation occurred. The assembly structure of CDFs changes the entire size of CDs, which influences the fluorescence. Meanwhile, the nearby CDs marked the fluorescence of each other. As well as this, surface chemistry plays an important role in fluorescence properties. The nitrogen atoms and sulfur atoms on the surface of CDs can generate energy traps. The bright fluorescence of CDs attributes to the defect surface with many carbonyl and amino groups. After the functionalization of PEI, the surface of CDFs was dominated by the amino groups, which quenched the fluorescence together with the growing sizes as well as the marking effects of the nearby CDs. The comparison of the fluorescence behavior of CDs and CDFs was further examined by Time-correlated single-photon counting (TCSPC) to understand the photo-generated charge recombination pathways of the materials (Fig. 4b). Emission was monitored at 430 nm. The fluorescence decays required a two-component exponential fit. The time constants and relative amplitudes are fitted and summarized in Table S1. It could be seen that the lifetime of the dominant component for CDs was 2.45 ns, while that of the other component was 7.47 ns. On the other hand, the lifetime of the dominant component for CDs was 1.98 ns while the other component showed a lifetime of 7.30 ns. No significant lifetime change was observed between CDs and CDFs, which also indicated the properties of CDs was not substantially changed while assembly into CDFs [18]

3.2. Toxicity

For evaluation of the safety of the materials, the toxicity of the CDs and CDFs to PC12 cells are investigated. Assays of 3-(4, 5-Dimethylthiazol-2-yl)-2, 5-diphenyltetrazolium bromide (MTT) were conducted to investigate the influence of the materials on cell viabilities (Fig. 5). After incubation of PC12 with CDs and CDFs, cell viabilities were not much affected within 24 hours. Interestingly, both carbon materials promote the proliferation of PC12, which plays an important role in the therapy of nerve damage. These results indicate the low toxicity of the materials and the materials are promising for nerve protections with PC12 cells involved. [19]

3.3. Antibacterial investigations

The antibacterial activities of the CDs and CDFs were initially evaluated by measuring the bacterial density in the presence of these agents at 600 nm. [20] As shown in Fig. 6, the results suggest a substantial antibacterial effect of both the CDs and CDFs against both the *S. aureus* and *E. coli* cells. Especially, the cell viability of the *S. aureus* cells was almost 0 when larger than 30 μg/mL of the CDFs were used. Similarly, the *E. coli* cells were disinfected by both CDs and CDFs. Based on the zeta potential investigations, CDs showed multiple charges. On the other hand, the CDFs were with insignificant charges, which might suppress the bacterial adhesion under weak repulsion thus interacting with the bacterial surface more easily. By comparison, the CDFs show higher antibacterial activity based on the phenomena that a relatively larger ratio of the cells are killed when larger than 6 μg/mL of the materials

are used. The enhanced antibacterial activity of CDFs is possibly attributed to the synergy effect of CDs as building blocks as well as the more stable surface charges.

To further confirm whether the integrity of the bacterial membrane was damaged upon the CDs and CDFs treatment, the live/dead staining experiment was performed by using 30 μg/mL of these agents (Fig. 7). The green fluorescent FDA staining can only show the live cells while red fluorescent PI can only stain dead bacteria with broken membranes, but the live ones with intact bacterial membranes are unstained. [21] As shown in the fluorescence images, obvious red fluorescence was seen in the CDs-treated samples and a much higher density of the dead cells was seen by the CDFs-treated samples.

Based on the above comparisons, we conclude that CDFs are more promising for killing both Gram-positive and Gram-negative bacterial cells. Therefore, *E. coli* and *S. aureus* before and after treating with 30 μg/mL of CDFs were characterized by SEM (Fig. 8). As shown in the Fig. 8a and 8c, bacteria before treatment with CDFs exhibit regular surface. However, after incubating with CDFs, the morphology of the bacterial cells including *S. aureus* (Fig. 8b) an*d E. Coli* (Fig. 8d) changed drastically. Moreover, the membranes of many bacterial cells broke apart. Some small materials were observed on the surface of the bacteria, which originated from the attached CDFs. This indicates the CDFs can disinfect the bacterial by damaging the membranes. [22]

4. Conclusions

The assembly of CDs into CDFs result in more robust antibacterial activity. It is concluded that the assembly structure enables more stable properties but magnifies the antibacterial activity of CDs. This work also provides a new avenue of assembly small nanomaterials into frameworks for more practical applications.

Declarations

Declarations

5. Conflict of interest

The authors declare no conflict of interest.

Funding

This research was funded by the PhD. Start-up Fund of Science and Technology Department of Liaoning Province, China (201601363) and the Youth Fund of Education Department of Liaoning Province, China (JYTQN201712).

Author Contributions

Conceptualization, P.Z.; D.L.; methodology, P.Z.; software, P.Z.; K.L.; D. Y. L.; H.Q.; Y.E.; M.W.; X.M.; validation, P.Z.; K.L.; D. Y. L.; H.Q.; Y.E.; M.W.; J.S.; X.M.; D.L.; writing—original draft preparation, P.Z.; D.L.; funding acquisition, X.M. All authors have read and agreed to the published version of the manuscript.

8. Acknowledgments

The authors acknowledge Jinzhou Medical University for the instrument support.

References

1. Yinghan Chan XHW (2021) Buong Woei Chieng, Nor Azowa Ibrahim and Yoon Yee Then. Superhydrophobic Nanocoatings as Intervention against Biofilm-Associated Bacterial Infections. Nanomaterials 11:1046. doi:10.3390/nano11041046
2. Leon-Buitimea A, Garza-Cardenas CR, Garza-Cervantes JA, Lerma-Escalera JA, Morones-Ramirez JR (2020) The Demand for New Antibiotics: Antimicrobial Peptides, Nanoparticles, and Combinatorial Therapies as Future Strategies in Antibacterial Agent Design. Front Microbiol 11:1669. doi:10.3389/fmicb.2020.01669
3. Shuai C et al. A strawberry-like Ag-decorated barium titanate enhances piezoelectric and antibacterial activities of polymer scaffold. Nano Energy 74, doi:10.1016/j.nanoen.2020.104825 (2020)
4. Wang L et al (2020) The Density of Surface Coating Can Contribute to Different Antibacterial Activities of Gold Nanoparticles. Nano Lett 20:5036–5042. doi:10.1021/acs.nanolett.0c01196
5. Kim TH et al (2020) Combating Antibiotic-Resistant Gram-Negative Bacteria Strains with Tetracycline-Conjugated Carbon Nanoparticles. Adv Biosyst 4:e2000074. doi:10.1002/adbi.202000074
6. Pinapati P, Joby JP, Cherukulappurath S (2020) Graphene Oxide Based Two-Dimensional Optical Tweezers for Low Power Trapping of Quantum Dots and E. coli Bacteria. ACS Applied Nano Materials 3:5107–5115. doi:10.1021/acsanm.0c00367
7. Wang Y, Yang Y, Shi Y, Song H, Yu C (2020) Antibiotic-Free Antibacterial Strategies Enabled by Nanomaterials: Progress and Perspectives. Adv Mater 32:e1904106. doi:10.1002/adma.201904106
8. Rawson TM, Ming D, Ahmad R, Moore LSP, Holmes AH (2020) Antimicrobial use, drug-resistant infections and COVID-19. Nat Rev Microbiol 18:409–410. doi:10.1038/s41579-020-0395-y
9. Sun B et al (2021) Insight into the effect of particle size distribution differences on the antibacterial activity of carbon dots. J Colloid Interface Sci 584:505–519. doi:10.1016/j.jcis.2020.10.015
10. Xie Y, Zheng W, Jiang X (2020) Near-Infrared Light-Activated Phototherapy by Gold Nanoclusters for Dispersing Biofilms. ACS Appl Mater Interfaces 12:9041–9049. doi:10.1021/acsami.9b21777

11. Li D et al (2020) Development of coinage metal nanoclusters as antimicrobials to combat bacterial infections. J Mater Chem B 8:9466–9480. doi:10.1039/d0tb00549e
12. Ergene C, Yasuhara K, Palermo EF (2018) Biomimetic antimicrobial polymers: recent advances in molecular design. Polymer Chemistry 9:2407–2427. doi:10.1039/c8py00012c
13. Wang H et al (2021) Carbon dots with positive surface charge from tartaric acid and m-aminophenol for selective killing of Gram-positive bacteria. J Mater Chem B 9:125–130. doi:10.1039/d0tb02332a
14. Dong X et al (2020) Photoexcited state properties and antibacterial activities of carbon dots relevant to mechanistic features and implications. Carbon 170:137–145. doi:10.1016/j.carbon.2020.08.025
15. Boobalan T et al (2020) Mushroom-Derived Carbon Dots for Toxic Metal Ion Detection and as Antibacterial and Anticancer Agents. ACS Applied Nano Materials 3:5910–5919. doi:10.1021/acsanm.0c01058
16. Zhang E et al (2020) Carbon Dots@rGO Paper as Freestanding and Flexible Potassium-Ion Batteries Anode. Adv Sci (Weinh) 7:2000470. doi:10.1002/advs.202000470
17. Zapata RO et al (2008) Confocal laser scanning microscopy is appropriate to detect viability of Enterococcus faecalis in infected dentin. J Endod 34:1198–1201. doi:10.1016/j.joen.2008.07.001
18. Nguyen HA, Srivastava I, Pan D, Gruebele M (2020) Unraveling the Fluorescence Mechanism of Carbon Dots with Sub-Single-Particle Resolution. ACS Nano 14:6127–6137. doi:10.1021/acsnano.0c01924
19. Sobhanan J et al (2020) Toxicity of nanomaterials due to photochemical degradation and the release of heavy metal ions. Nanoscale 12:22049–22058. doi:10.1039/d0nr03957h
20. Shen Z et al (2020) Biomembrane induced in situ self-assembly of peptide with enhanced antimicrobial activity. Biomater Sci 8:2031–2039. doi:10.1039/c9bm01785b
21. Hu C et al (2020) Dual-responsive injectable hydrogels encapsulating drug-loaded micelles for on-demand antimicrobial activity and accelerated wound healing. J Control Release 324:204–217. doi:10.1016/j.jconrel.2020.05.010
22. Ju J et al. Designing Robust, Breathable, and Antibacterial Multifunctional Porous Membranes by a Nanofluids Templated Strategy. Adv Func Mater 30, doi:10.1002/adfm.202006544 (2020)

Unsectioned Paragraphs

1. **Introduction**

Bacterial infections show a serious threat to human lives and the development of effective medicines to disinfect bacteria are in great demand. [1] Various antibiotics have been used for treating bacterial infections, but the overuse of antibiotics causes other problems such as side effects and drug-resistant issues. [2] The nanomaterials including antimicrobial polymers, [3] metal nanomaterials, [4], and carbon nanomaterials [5,6] have been used as alternatives to classical antibiotics. [7] Both drug-resistant and toxic problems are relieving. [8] Recently, CDs [9] and nanoclusters (NCs) [10] are well applied for combating

bacterial infections because they are biocompatible, active, and can be easily cleaned by circulations due to the ultra-small sizes. [11,12] Especially, researchers have found that CDs show excellent free radical scavenging ability, which can be stronger than many traditional anti-infection drugs. [13–15] However, these ultra-small antimicrobials also suffer poor stability due to the larger oxidative surface area. [16] It is highly desired to develop more effective antibacterial agents for combating bacterial infections for long-term use.

To meet the demand for practical applications, the antimicrobials should have the following characteristics: a) Excellent stability remains unchanged for a certain time in an ambient environment; b) Excellent biocompatibility and low toxicity: c) high antibacterial activity. The larger nanomaterials are more stable, but relatively weaker antibacterial activity tends to be exhibited due to the smaller active surface area. Considering both the weakness of small and large nanomaterials, we report the assembly of the small CDs into large CDFs by simply adding polyethyleneimine (PEI) (Fig. 1). CDs were not fused but kept their morphology as building blocks. Therefore, the entire CDFs showed larger sizes but demonstrated more excellent stability without losing the active properties of CDs. Further, we found the CDFs displayed enhanced antibacterial activities against both Gram-negative Escherichia coli (*E. coli*) and Gram-positive Staphylococcus aureus (*S. aureus*) compared to CDs, indicating their broad-spectrum antibacterial performance. This work suggests the assembly of small CDs into large CDFs not only enhances the stability but also magnify the antibacterial activity.

Supplementary Material

The following are available online at www.mdpi.com/xxx/s1, Figure S1: TEM (a) and AFM (b) of the as-obtained CDs; Figure S2: (a) UV-vis, (b) the fluorescence excitation and emission spectra of the CDs; Figure S3: XPS survey (a) and FTIR of the as-obtained CDs; Table S1: Lifetime of the CDs and CDFs.

Figures

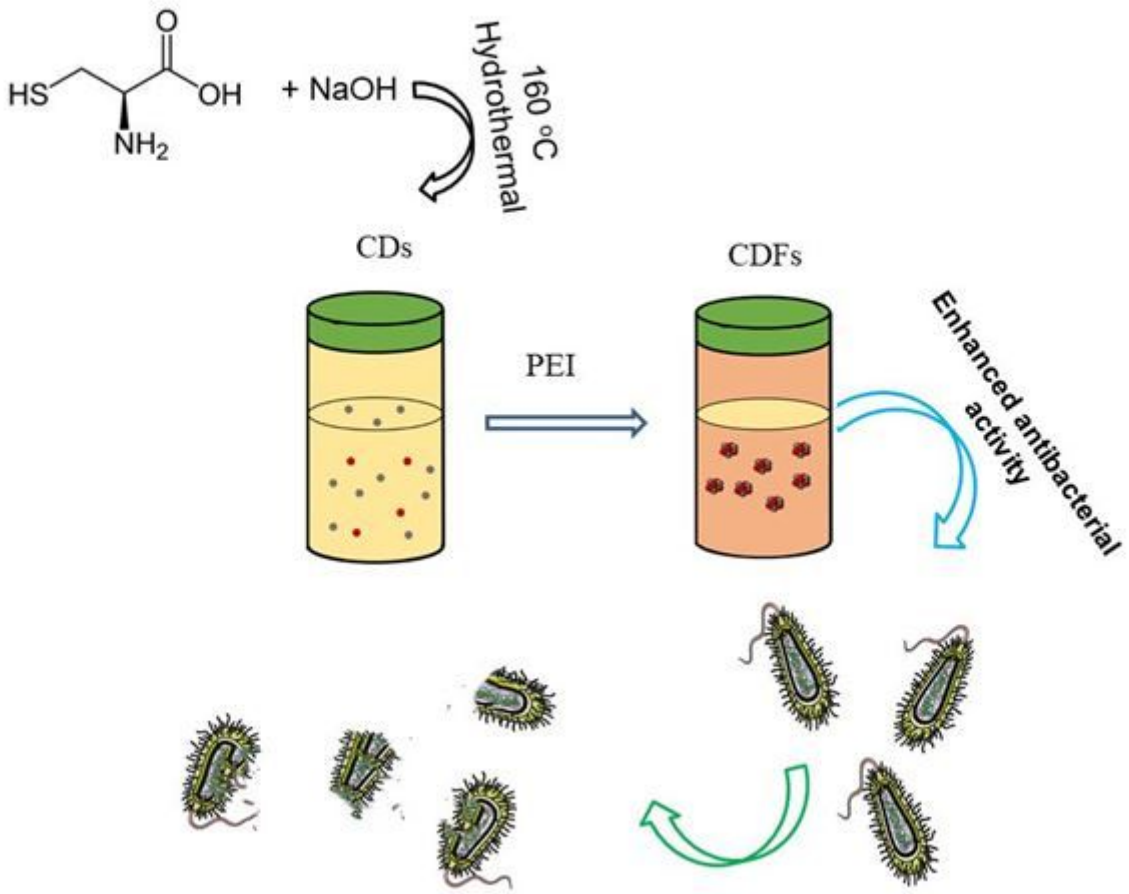

Figure 1

Scheme for the synthesis of CDs and the assembly into CDFs by adding PEI with enhanced antibacterial activity.

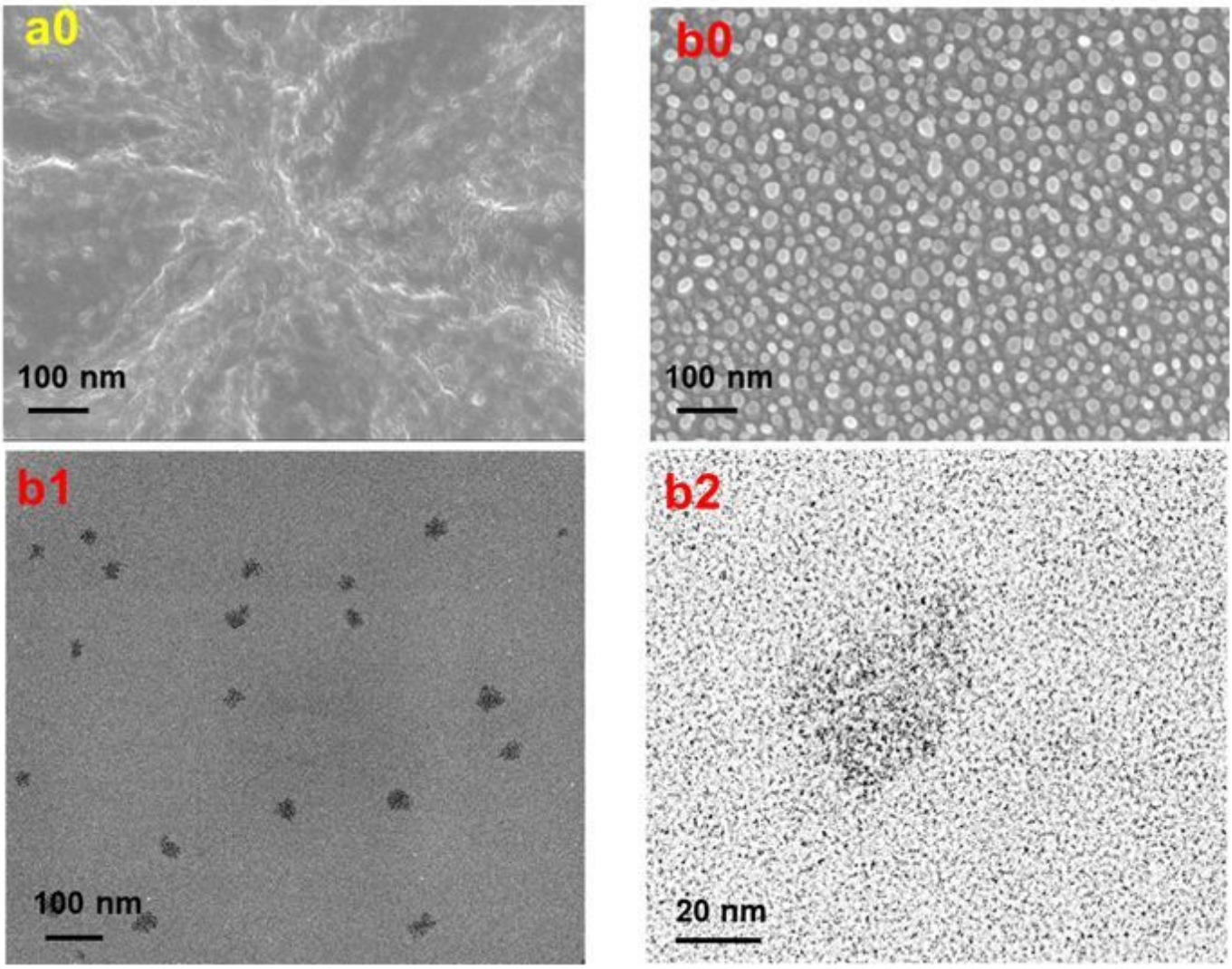

Figure 2

SEM for CDs (a), CDFs (b); TEM of relatively lower (b1) and higher magnification of CDFs.

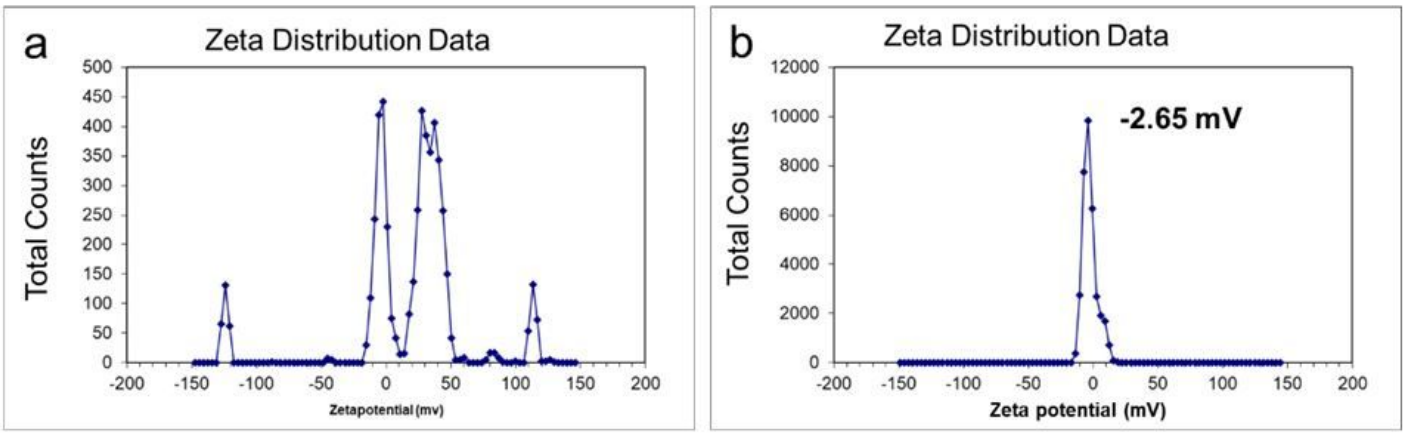

Figure 3

Zeta potential of CDs (a) and CDFs (b).

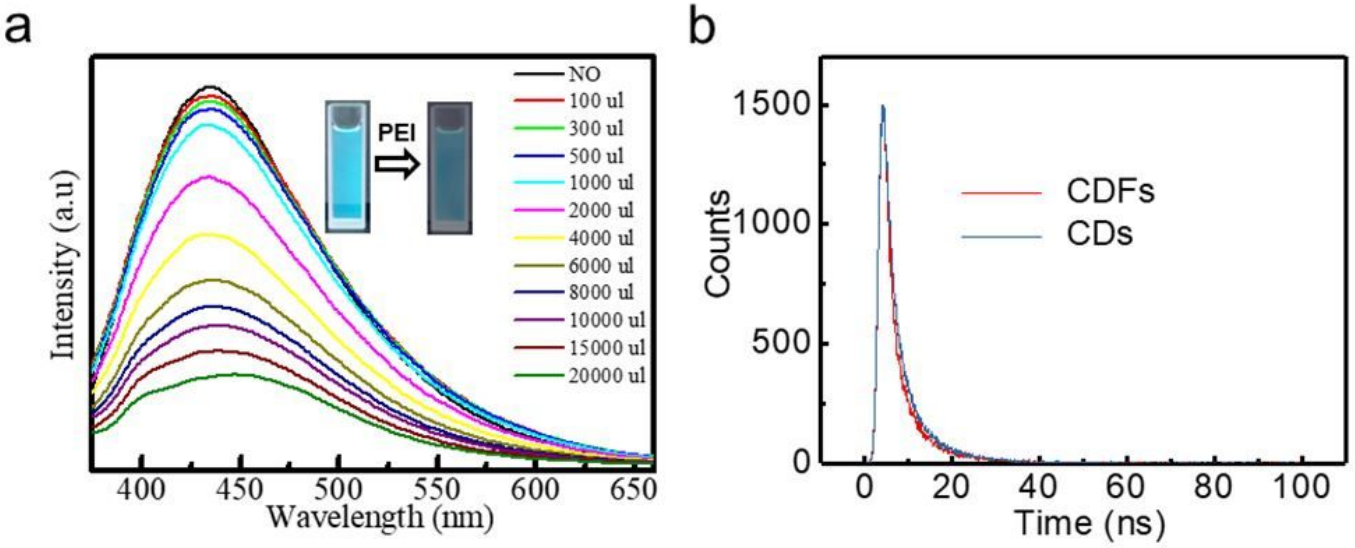

Figure 4

Fluorescence emission spectra (a) of CDs as the titration of PEI, and lifetime (b) for CDs and CDFs.

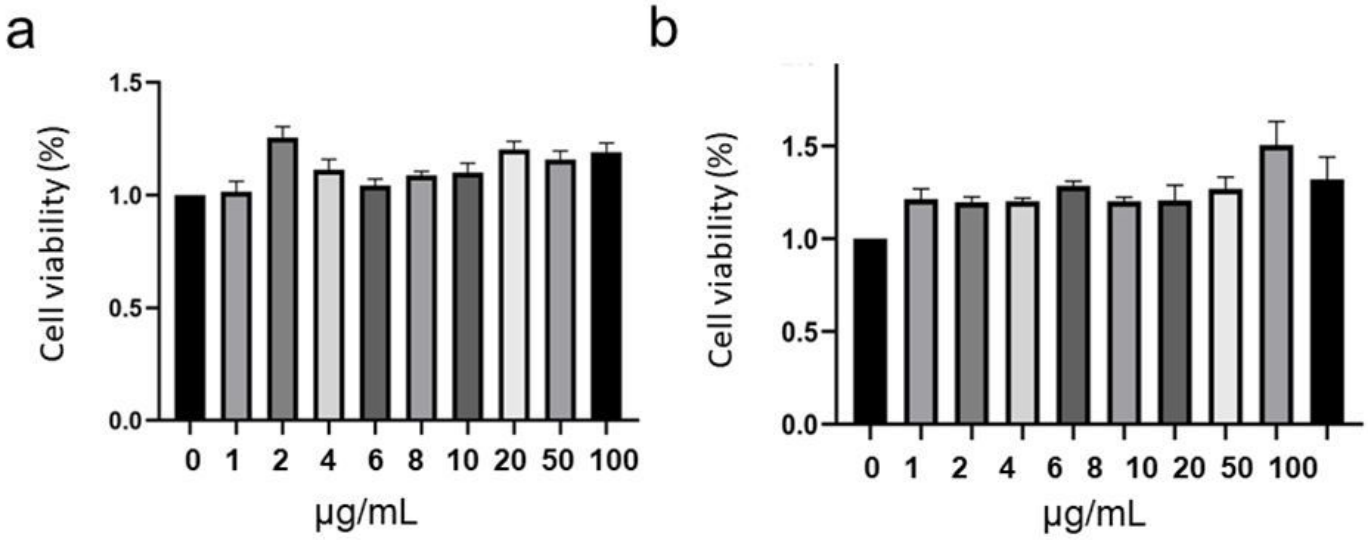

Figure 5

Cell viability of PC12 in the presence of CDs (a) and CDFs (b). Cell viability (%) = (absorbance of the experimental group - absorbance of the blank group)/(absorbance of the control group - absorbance of the blank group) × 100%.

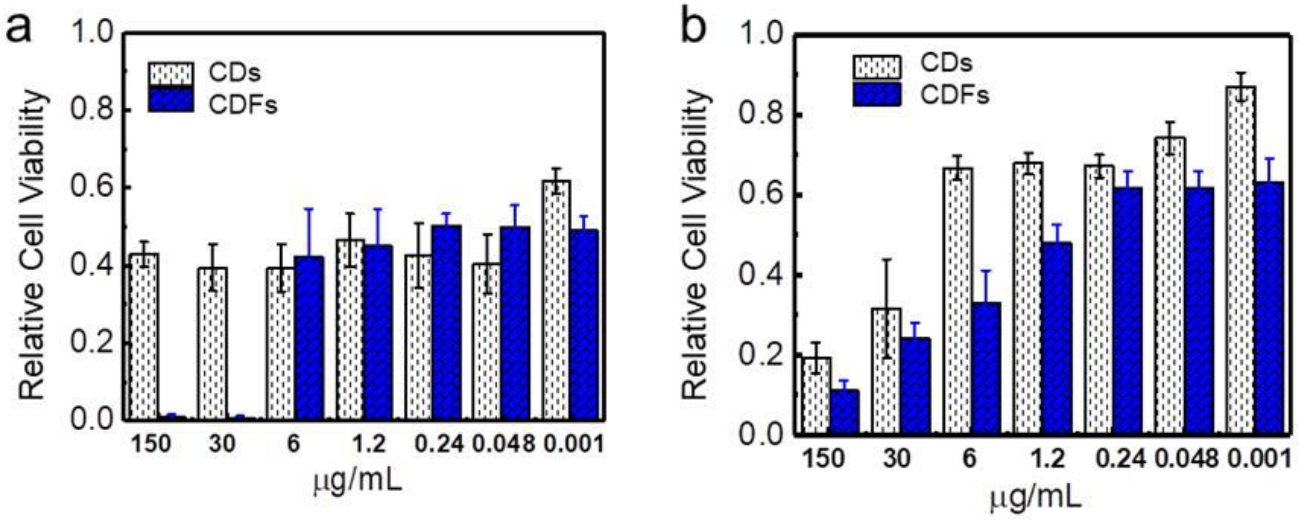

Figure 6

Antibacterial activity of CDs and CDFs against S. aureus (a) and E.coli (b).

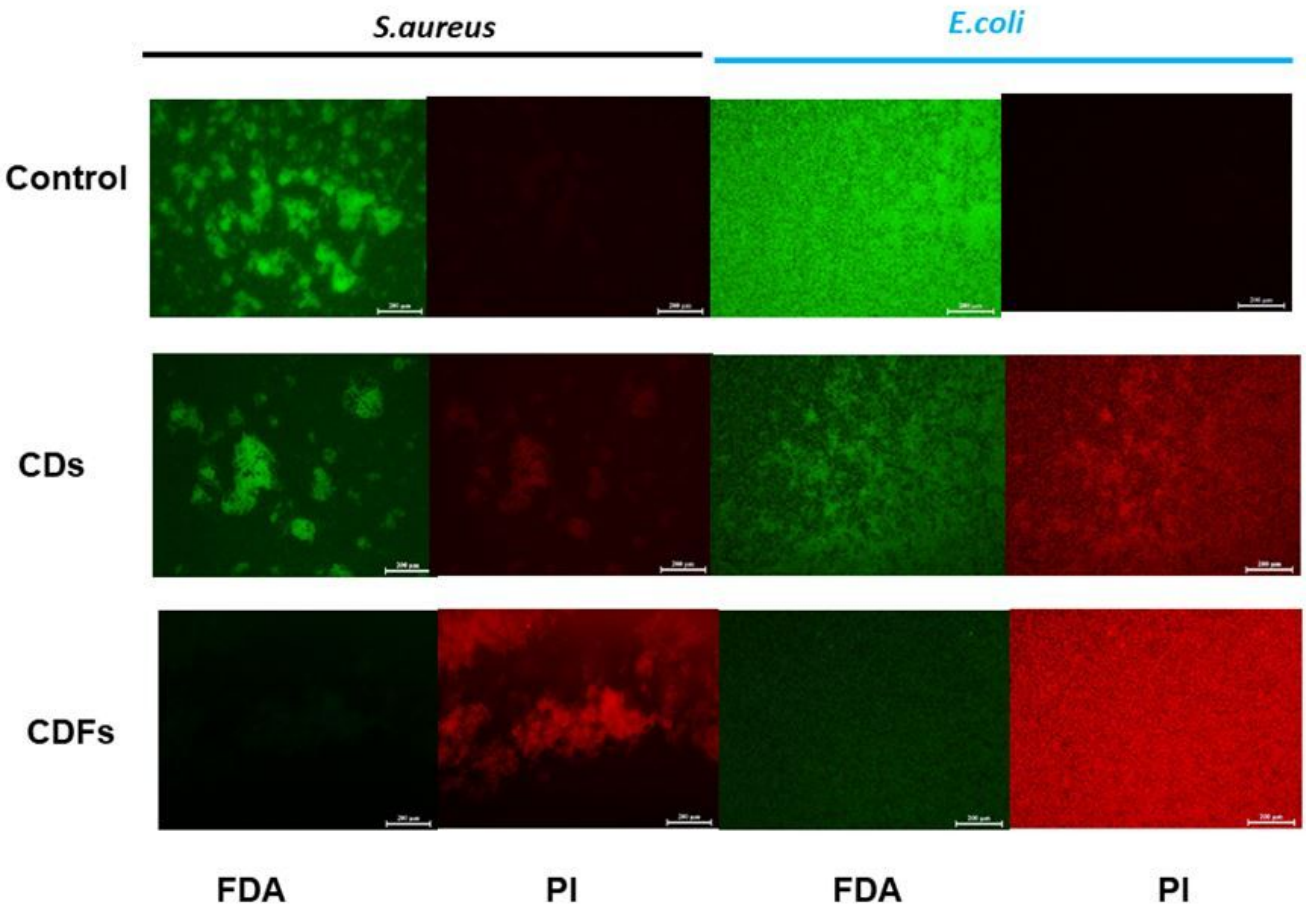

Figure 7

FDA/PI staining S. aureus and E. coli in the absence and presence of CDs and CDFs. Scale bar, 200 μm.

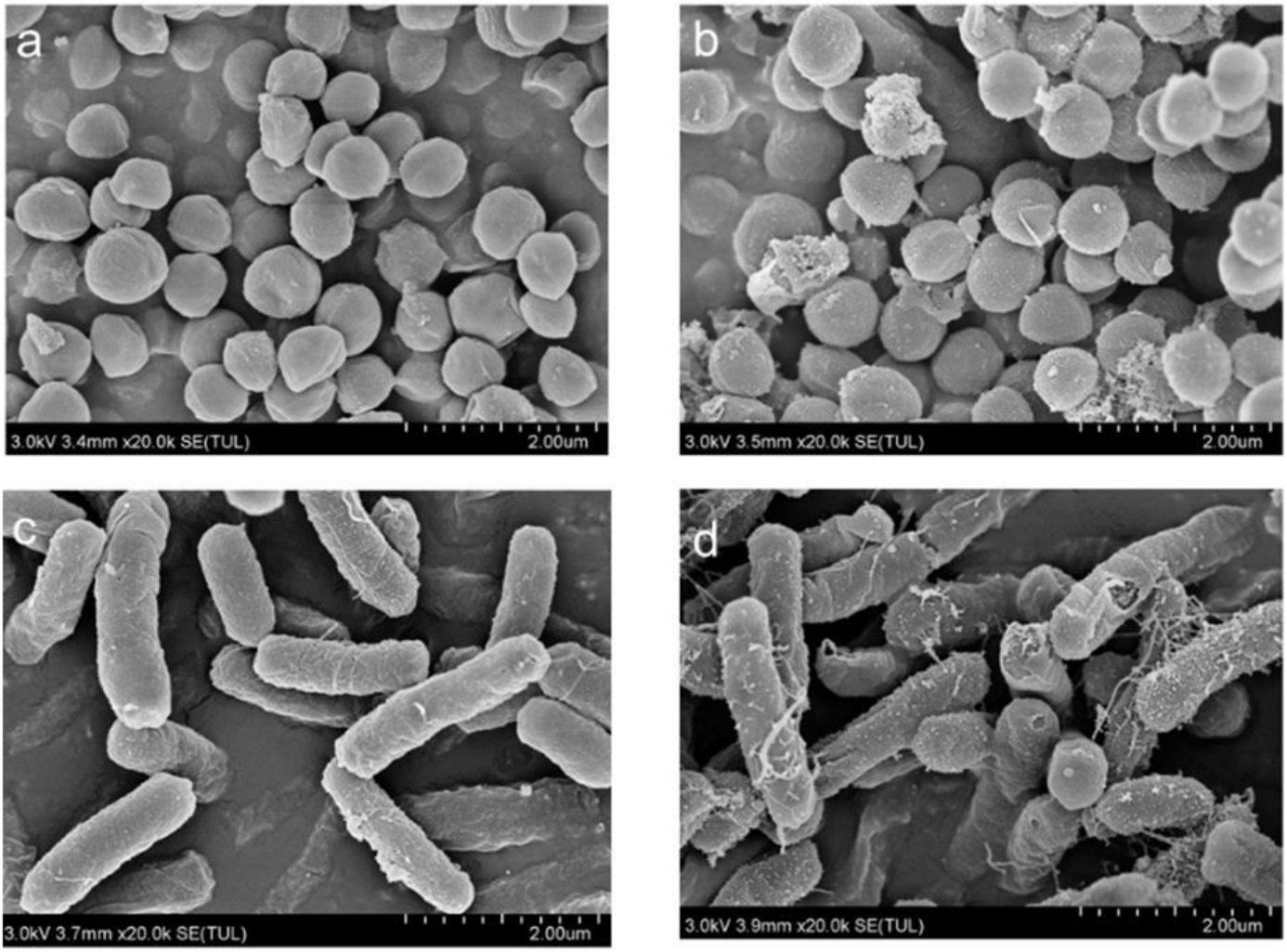

Figure 8

SEM for S. aureus (a, b) and E.coli before (a, c) and after (b, d) the treatment with 30 μg/mL of CDFs. Scale bar: 2 μm.Additional Requirements

Supplementary Files

This is a list of supplementary files associated with this preprint. Click to download.

- SupportinginformaitonFinal.docx